WESTINGHOUSE CLASS 3

WCAP-9663

METALLURGICAL INVESTIGATION OF CRACKS IN THE PRESSURIZER NOZZLE-TO-SAFE-END WELD OF THE ROBERT EMMETT GINNA NUCLEAR POWER GENERATING STATION

G. V. Rao
J. S. Caplan

February 1980

APPROVED: T. R. Mager

T. R. Mager, Manager
Metallurgical and NDE Analysis

Work Performed Under Shop Order No. RHN-52072

WESTINGHOUSE ELECTRIC CORPORATION
Nuclear Energy Systems
P. O. Box 355
Pittsburgh, Pennsylvania 15230

ABSTRACT

This report describes the results of a metallurgical investigation into the cracking of the pressurizer relief nozzle-to-safe-end weld of the Robert Emmett Ginna Nuclear Power Generating Station. The cracks were first discovered during liquid penetrant tests as part of the ISI program. The metallurgical evaluations performed on a boat sample containing cracks included metallographic and fractographic examinations, fine structure studies, chemical evaluations, and delta ferrite content measurements of the weld metal.

The tests showed that the cracks were situated in the Type 309 stainless steel weld metal close to the carbon steel/weld metal interface. The cracks appear to have initiated on the outside surface and grew radially inward, the deepest crack being measured approximately at .04 inch. The general orientation of cracks on the surface of the weld followed the circumferential direction of the nozzle-to-safe-end pipe assembly. The cracks were intergranular in nature. EDAX and SEM evaluations of the fracture faces did not reveal any evidence of corrosion deposits. Light optic color photographic evaluations of the crack faces showed that the fracture faces were heavily covered with a high-temperature metal-oxide film. Fine structure studies indicated no significant evidence of any intergranular carbide precipitation, while the delta ferrite content measurements showed significantly lower amounts of delta ferrite (2.5% to 3%) content in the weld metal close to the interface. It was further observed that the physical location of the cracks in the nozzle-to-safe-end weld assembly corresponded to the region of a geometric discontinuity where high local strains due to restraint conditions are likely to be present. On the basis of these observations it is believed that the observed cracking is most likely the result of super solidus cracking or "hot cracking." The low delta ferrite content of the weld metal and the appreciable local strains that are likely to be present due to geometrical discontinuity at the location of the cracks are considered to be among the factors contributing to the cracking process.

The cracking is considered to be due to excessive dilution of weld metal local to the weld interface, resulting in unusually low delta ferrite contents not normally encountered in these welds. The role of delta ferrite is generally well understood and the chemistry of the weld metal is well controlled to produce adequate delta ferrite contents to avoid hot cracking. For these reasons, the current cracking incident should be considered exclusively local and not a generic one, and should not warrant any safety concerns.

TABLE OF CONTENTS

LIST OF ILLUSTRATIONS

SECTION 1.0
INTRODUCTION

This report summarizes the findings of a metallurgical investigation into the cracking of the pressurizer relief nozzle-to-safe-end weld of the Robert Emmett Ginna Nuclear Power Generating Station. Indications were first observed on the pressurizer nozzle-to-safe-end assembly during liquid penetrant examination by RGE personnel as part of the ISI program. Further examination by replicating tape revealed (see reference 1) that the cracks existed in the Type 309 weld metal close to the nozzle safe end. A boat sample was removed along the circumferential direction of the weld containing several cracks, stainless steel weld metal, and carbon steel base material, and was sent to Westinghouse for further evaluation and metallurgical investigations. A schematic diagram of the pressurizer relief nozzle-to-safe-end assembly showing the location of the cracks and the boat sample is illustrated in figure 1-1.

The metallurgical investigations included the following tasks:

- Surface and metallographic examination of various sections of the boat sample containing the cracks.
- Microstructural characterization studies of the weld metal by light optic and thin foil electron microscopy techniques.
- Metallographic estimates of delta ferrite content of the weld metal.
- Fractographic examinations of the fracture faces by light optic color photography and scanning electron microscopy techniques.
- Chemical evaluations of the crack faces and of the deposits by Energy Dispersive x-ray (EDAX) analysis and microprobe trace analysis techniques.

The results of these tasks are presented in the following sections.

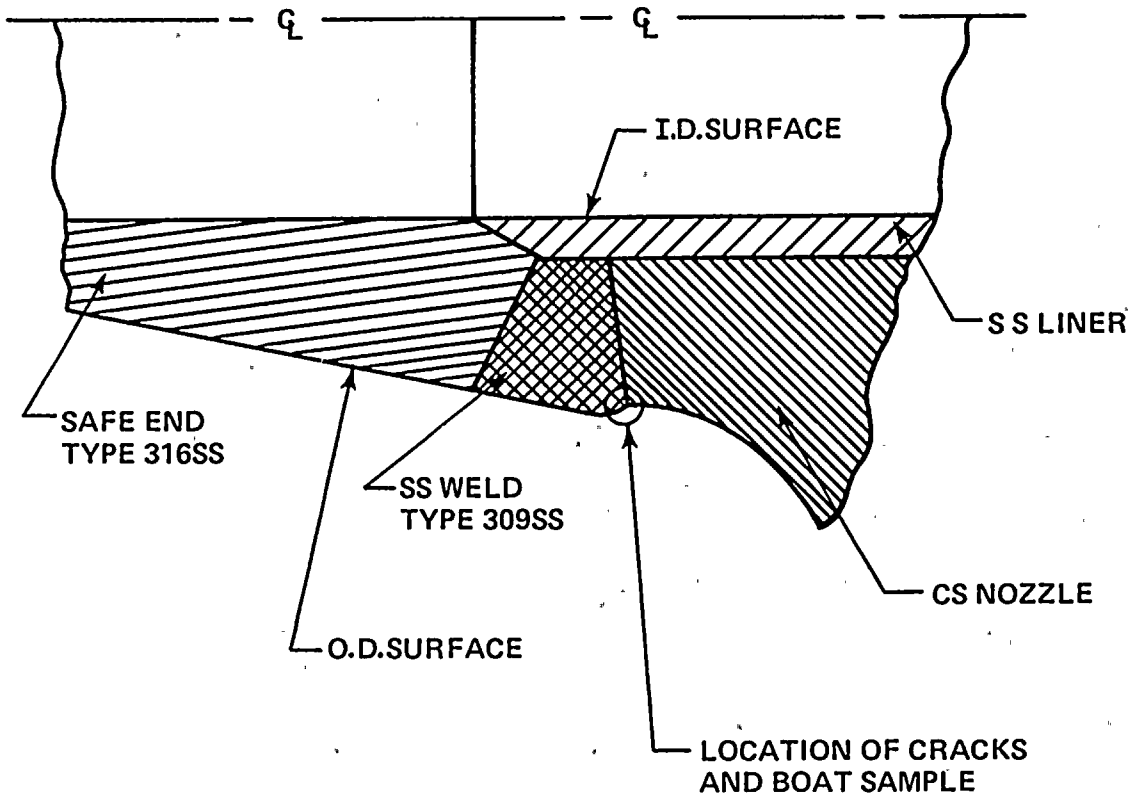

Figure 1-1. Schematic of RGE Pressurizer Relief Nozzle-to-Safe-End Weld Assembly Showing the Location of Cracks and the Boat Sample

SECTION 2.0

EXAMINATIONS AND TESTS

2.1 SURFACE EXAMINATIONS AND EVALUATION PROCEDURE

The boat sample was first surface polished and carefully examined by light microscopy prior to its sectioning in order to establish the location and distribution of cracks. The boat was then sectioned at two selected locations to produce three specimens designated as A, B, and C which were employed for various aspects of metallurgical investigation as illustrated in figure 2-1. The first cut was taken through the region containing the largest population of surface cracks so that an accurate assessment of morphology and distribution of cracks could be made from the resulting sections. The corresponding specimens A and B were employed respectively for fractographic and optical metallographic studies of the cracks. The specimen C, resulting from a second cut of the boat sample, contained essentially no cracks and was employed exclusively for the preparation of thin foil specimens of the weld metal for fine structure studies by transmission electron microscopy.

2.2 METALLOGRAPHY

2.2.1 Morphology and Distribution of Cracks

Specimen B from the boat sample which contained some of the deepest cracks was metallographically polished and examined to study the morphology and distribution of cracks. The metallography was conducted both on the OD surface of the specimen as well as on sections normal to the cracks. Optical micrographs of the cracks on the two planes are shown in figures 2-2 and 2-3 respectively. Magnified views of the major cracks are also shown in figures 2-4 and 2-5. Figure 2-6 shows the distribution of a cluster of fine cracks seen on the top surface of the boat sample in unetched condition. The above micrographs clearly illustrate that the general nature of cracking is intergranular and that some cracks extend from the OD surface of the Type 309 stainless steel weld to as deep as the stainless steel/carbon steel interface. Detailed discussion of these results is considered in a later section.

2.2.2 Delta Ferrite Content Measurements

Estimates of delta ferrite content of the weld metal were made metallographically by examining several representative areas in the vicinity of cracks using a Leitz classimet. The specimen preparation procedure included a special etching technique to reveal sigma and delta ferrite phases selectively. A 10-percent NaCN electrolytic etch at 0.13 A/cm^2 was employed initially to reveal sigma phase. The specimen was then lightly polished and was etched electrolytically with 20 percent NaOH for 20 seconds to bring out the delta ferrite. Average values for the ferrite content based on measurement on a total of 50 fields each time, ranged from 2.5 percent to 3.0 percent. Optical micrographs illustrating the typical distribution of delta ferrite in the weld metal are shown in figure 2-7.

2.2.3 Studies on the Grain Boundary Carbide Precipitation by Thin Foil Transmission Electron Microscopy

Fine structure studies of the austentic grain boundaries of the weld metal were conducted by thin foil electron microscopy with the specific purpose to see if there is any evidence of extensive grain boundary carbide precipitation due to the possible effect of sensitization. Weld metal foils were prepared from specimen C of the boat sample, and the final thinning was conducted on a twin-jet electropolisher. The studies indicated no evidence of appreciable carbide precipitation although a few fine carbide precipitates are occasionally seen along the grain boundaries. Figure 2-8 illustrates the electron micrographs of the fine structures observed. The microscopy was conducted on a Phillips 200 electron microscope equipped with a 100 kv electron beam.

2.3 FRACTOGRAPHY

Specimens containing some of the deepest cracks were carefully opened in the laboratory to examine the fractographic features of fracture surfaces. The specimens were cut dry so as not to contaminate the cracks or remove any deposits. Both light-optic color fractography and scanning electron fractography were conducted.

2.3.1 Light Optic Color Photography

The freshly opened crack surfaces were examined under light microscope and the fractographic features were documented by color photo-fractography. The fracture faces revealed interesting metal oxide colors indicative of the temperatures to which crack surfaces may have been first exposed to the oxidizing environment. Figure 2-9 and 2-10 illustrate the appearance of the fracture faces. Noticeable are the intergranular fracture paths and a heavy metal oxide film covering the fracture faces. The dark colored band at the top of the fractograph shows heavier oxidation at the crack mouth, presumably due to higher temperatures of oxidation and/or higher accesibility of oxygen as compared to the deeper regions of the crack surface.

Another interesting observation is that islands of cohesive material bridging the two crack faces were present prior to the laboratory opening of the crack. This is clearly evidenced by the bright reflective areas both at the bottom of the fractograph (figure 2-10) and at isolated locations (indicated by arrows) on the fracture face where laboratory fracture occurred during the opening of the crack at room temperature. The implications of various fractographic features described here will be brought out in detail in the discussion section of the report.

2.3.2 Scanning Electron Microscope (SEM) Fractography

Scanning electron fractography was conducted on the freshly opened cracks to reveal the morphology of the fracture faces. The fractographic features are illustrated in figures 2-11 and 2-12. Figures 2-11a and 2-11b illustrate typical fractographic features of the field fracture surface, while figure 2-12 illustrates a dimpled ruptured region resulting from the laboratory fracture of the weld metal during the opening of the cracks.

2.4 CHEMICAL ANALYSIS

2.4.1 Energy Dispersive X-Ray (EDAX) Analysis

The fracture surface material and deposits, if any, were analyzed using energy dispersive x-rays. The results are shown in figure 2-13. The EDAX spectrum basically indicates weld metal chemistry, namely Fe, Cr, and Ni, and shows no evidence of corrosion products such as chlorides, sulphides, etc.

2.4.2 Electron Microprobe Analysis

Electron microprobe trace analysis was conducted across several grain boundaries on metallographic sections containing cracks. The purpose here was to see if there is any detectable chromium depletion existing along the grain boundaries due to a possible sensitization of the weld metal. No such depletion could be detected. Figure 2-14 shows the results of a probe analysis across two grain boundaries near the vicinity of a crack.

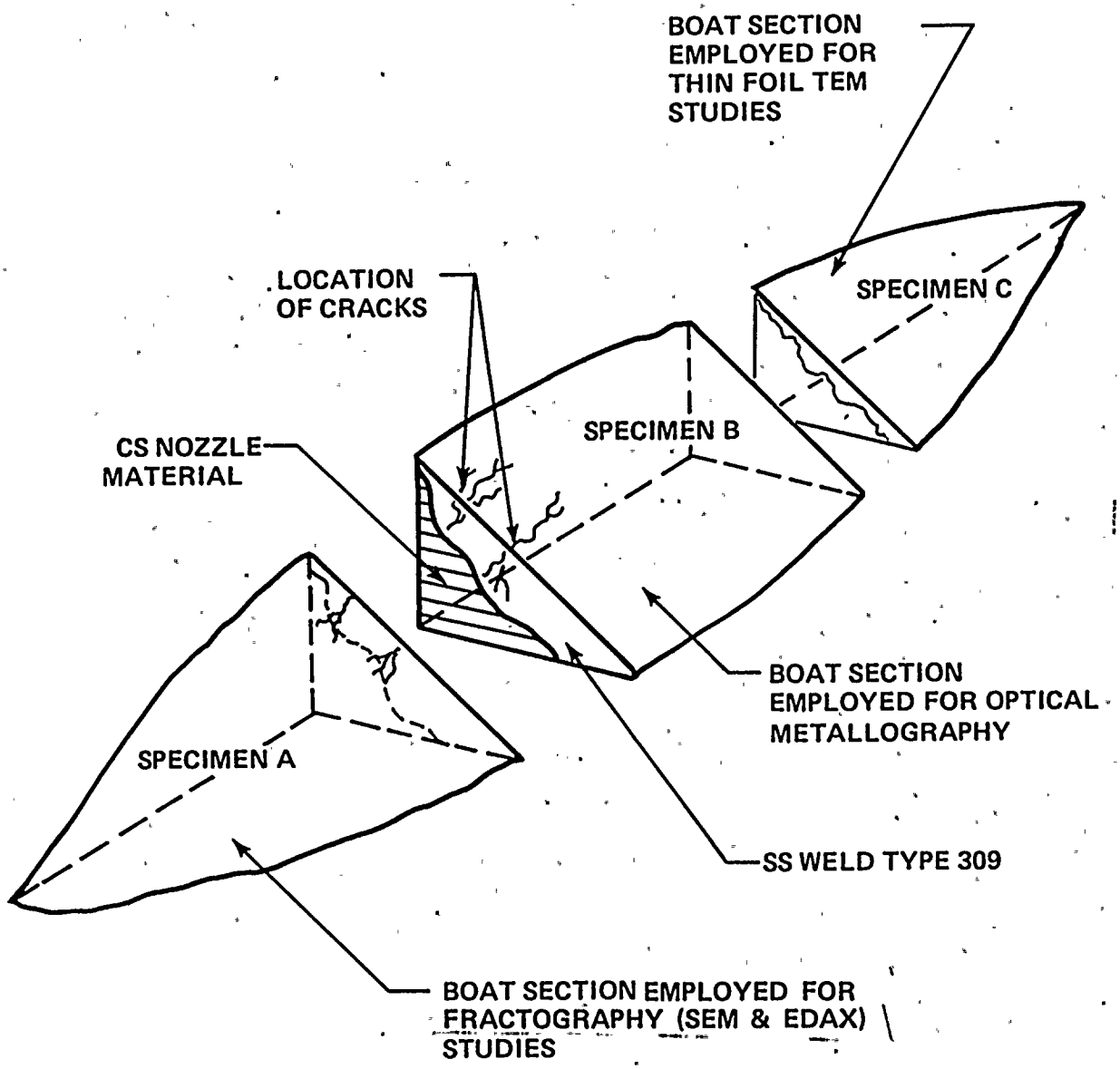

Figure 2-1. Schematic of Sectioned Boat Sample Employed for Various Aspects of Metallurgical Investigation

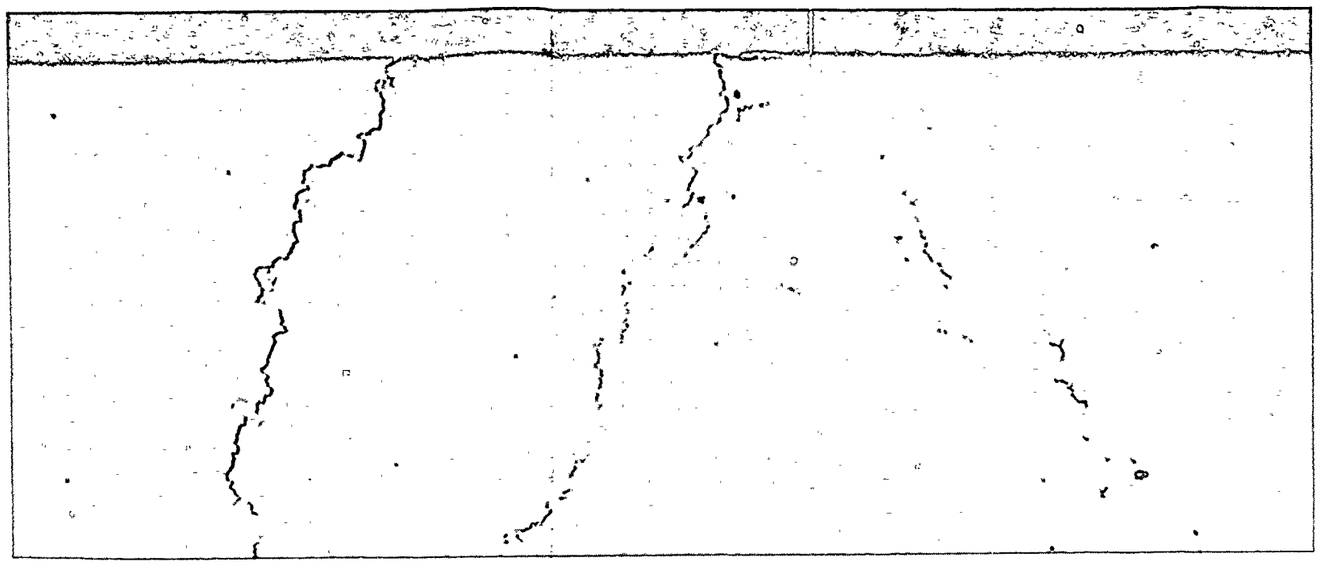

3 (a) 50X

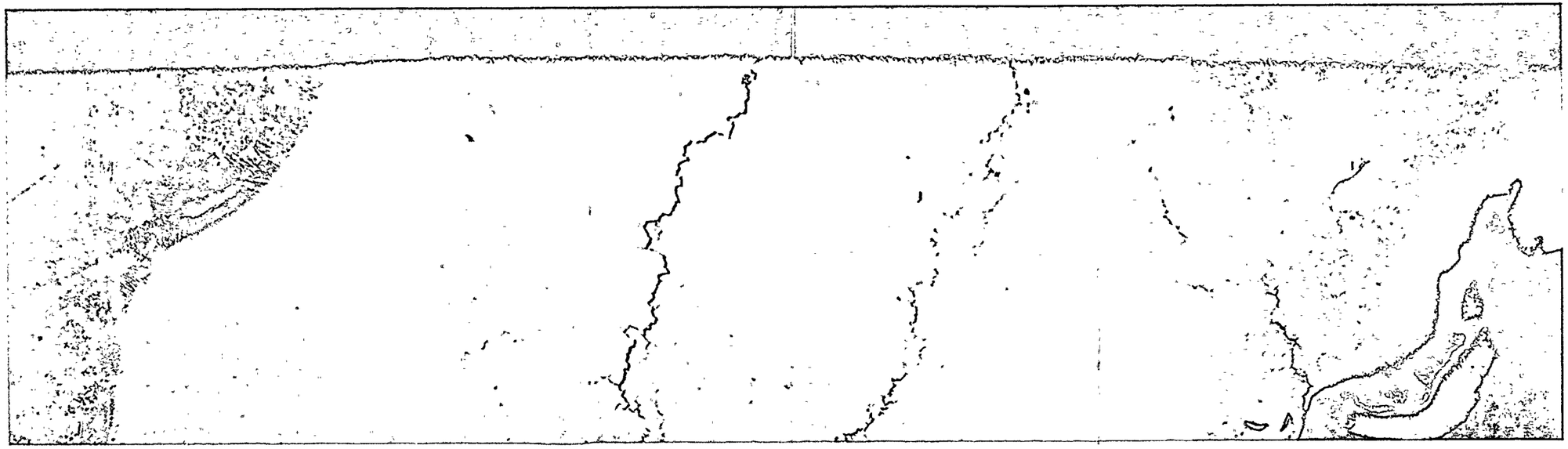

3 (b) 50X

Figure 2-2. Light Optical Micrographs Showing Morphology and Distribution of Cracks on a Section Parallel to the Surface of the Boat Sample; (a) Unetched, (b) Etched With 10% Oxalic

16000-2

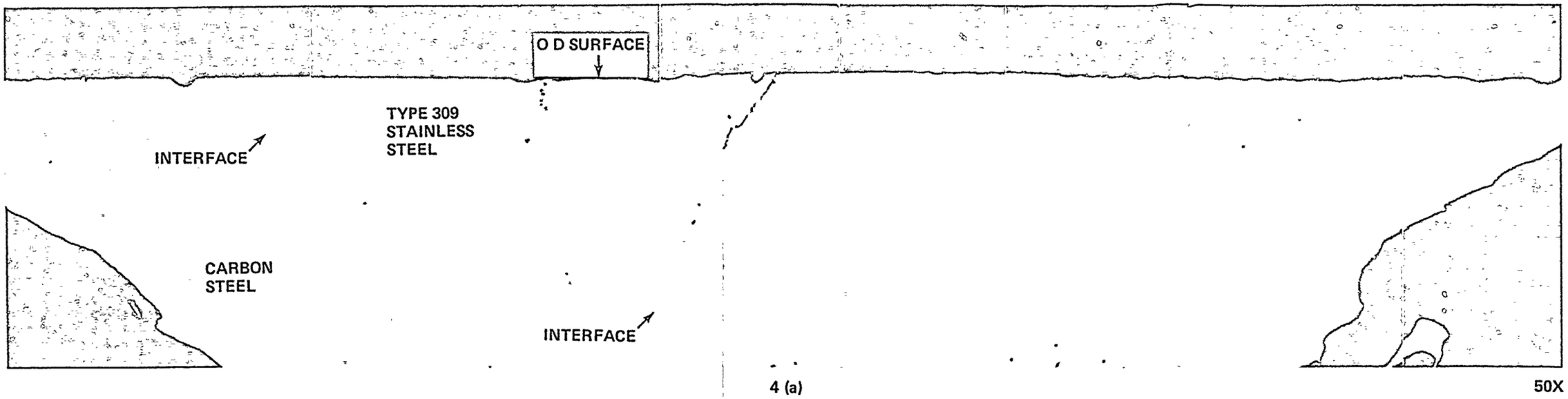

4 (a) 50X

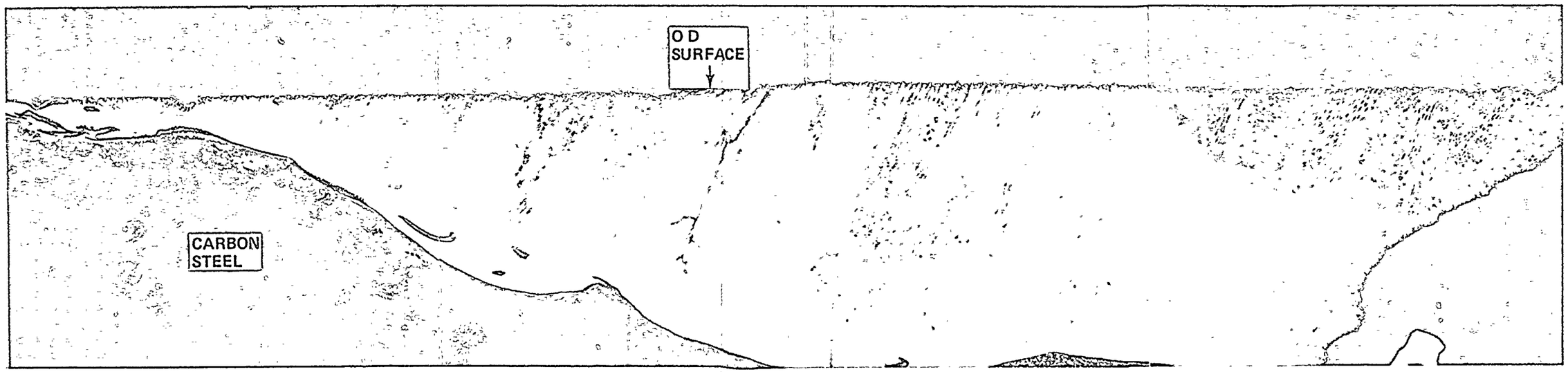

4 (b) 50X

Figure 2-3. Optical Micrographs Showing the Morphology and Distribution of Cracks on a Section of the Boat Sample Normal to the Cracks; (a) Unetched, (b) Etched with 10% Oxalic

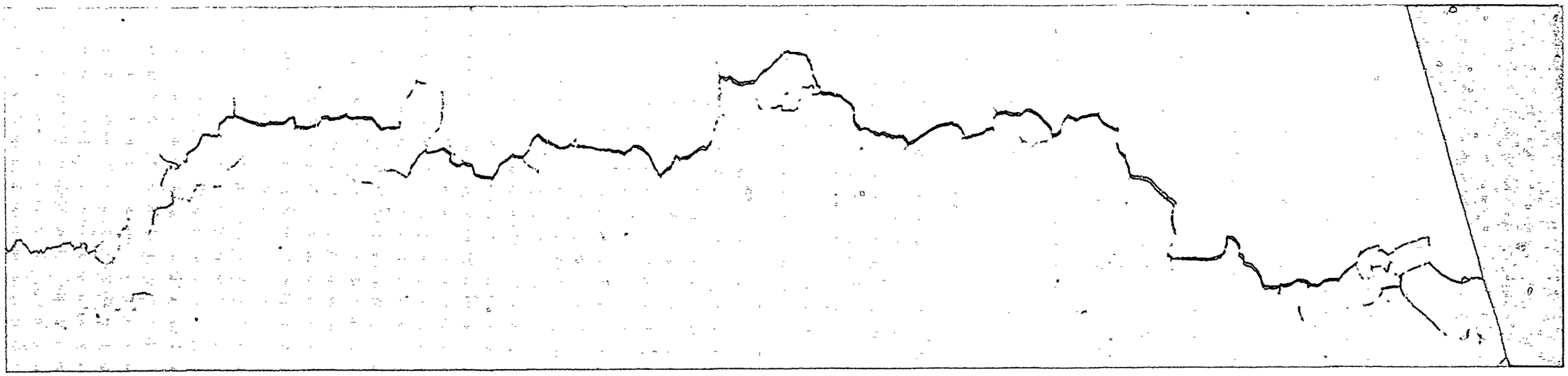

6 (a)

200X

LONGITUDINAL DIRECTION OF THE BOAT SAMPLE

CIRCUMFERENTIAL DIRECTION OF THE NOZZLE–SAFE-END WELD

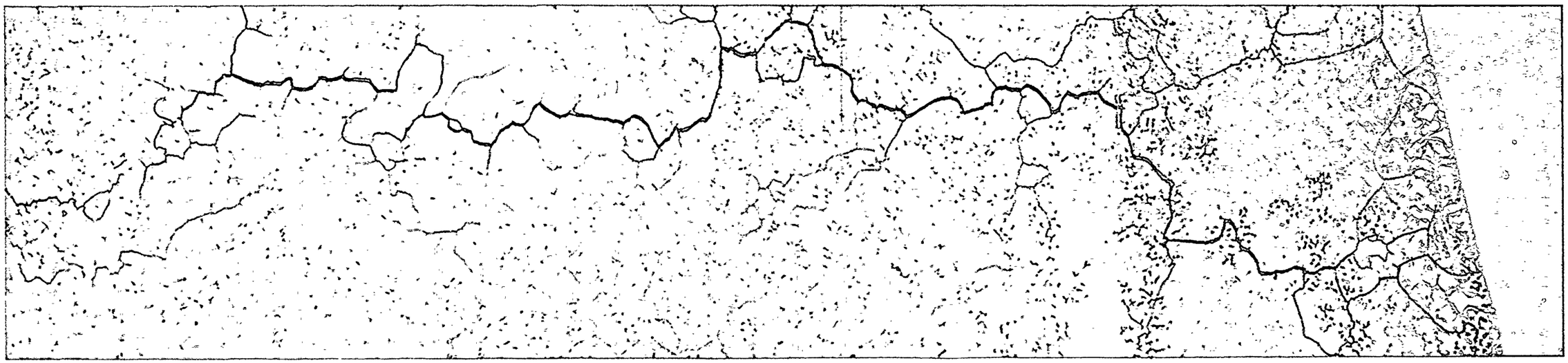

6(b)

200X

Figure 2-4. Optical Micrograph Showing the Largest Crack on the Surface (OD Surface of Nozzle-to-Safe-End Weld) of Boat Sample; (a) Unetched, (b) Etched Condition

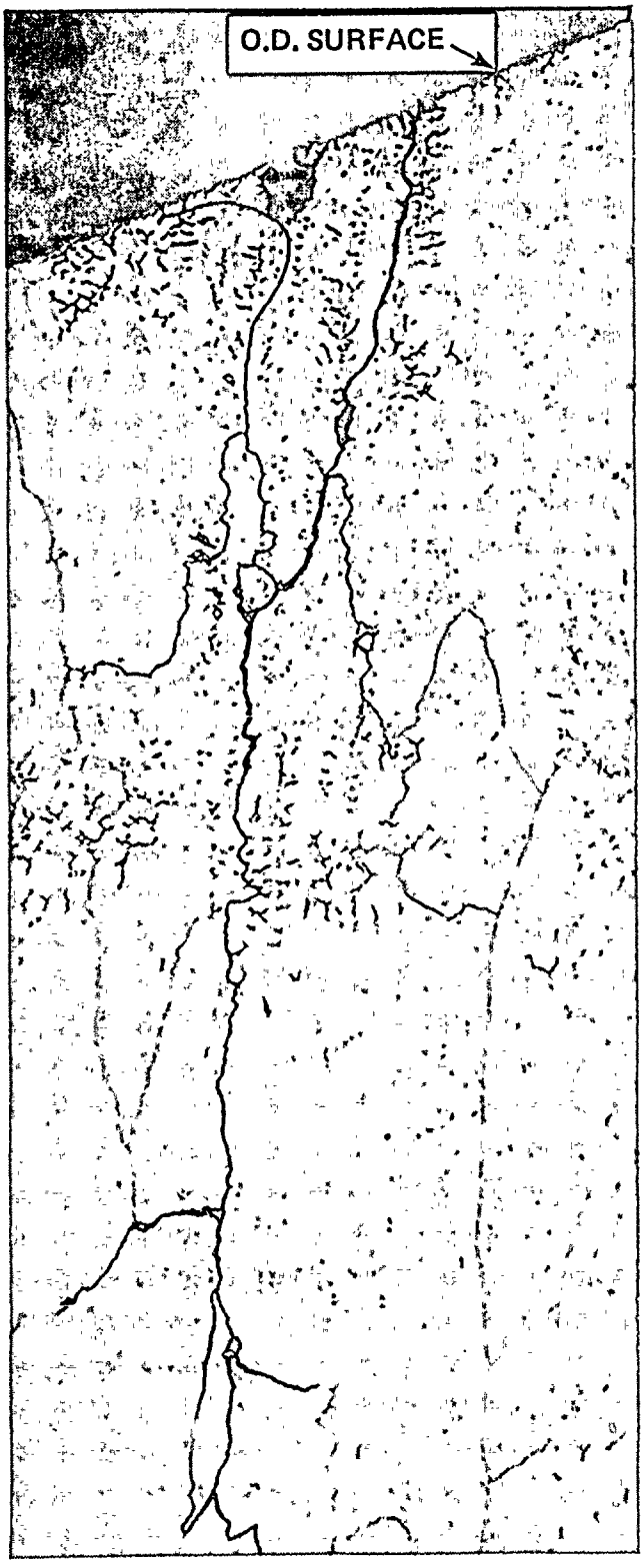

200X

Figure 2-5. Metallographic Section Containing the Deepest Crack, Shown at Higher Magnification

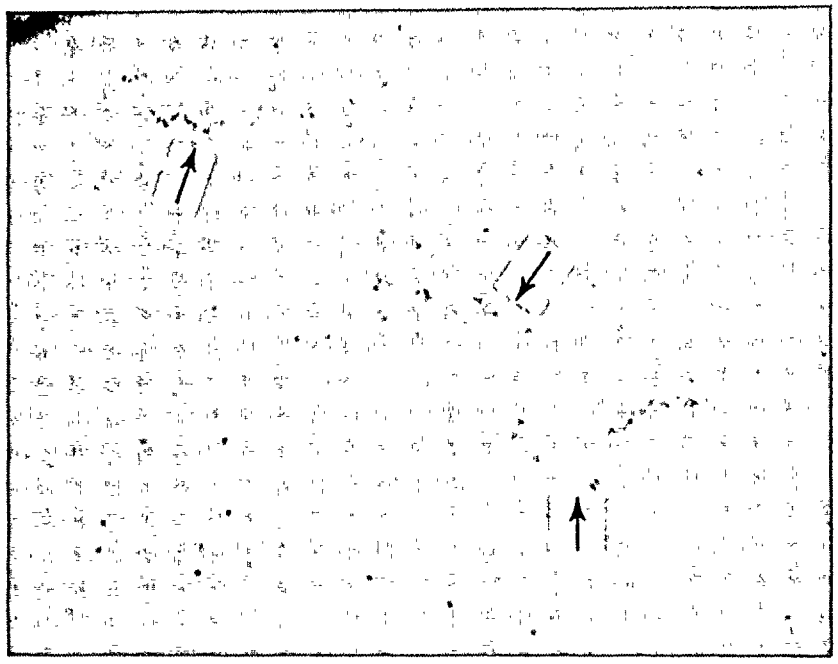

50X

Figure 2-6. Optical Micrograph (Unetched Condition) Showing the Distribution of Fine Cracks on the OD Surface

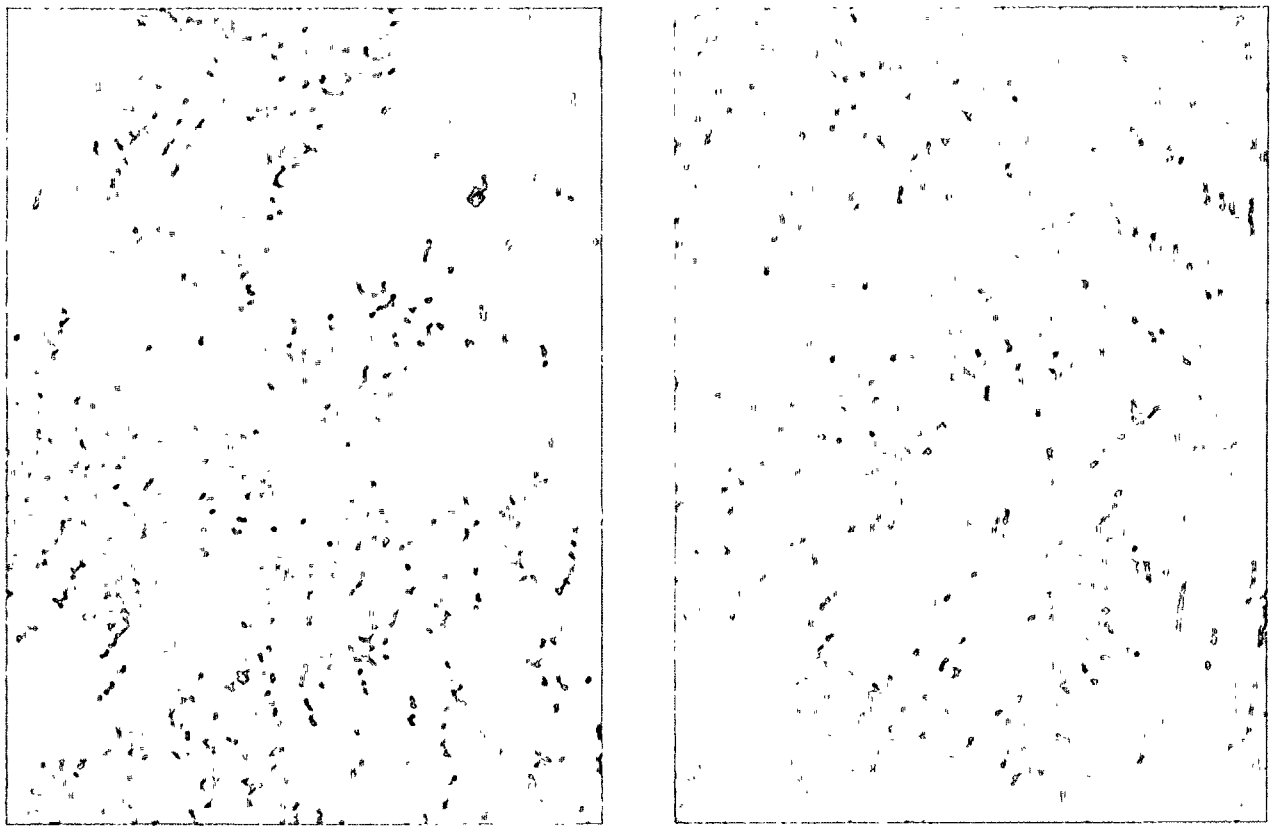

200X 200X

Figure 2-7. Optical Micrographs Showing the Distribution of Delta Ferrite in the Weld Metal (Electrolytic Etch With 20% NaOH). The Ferrite Content is Estimated to be in the Range Between 2.5 and 3 Percent

37000X

a) FINE STRUCTURE WITHIN AUSTENITE

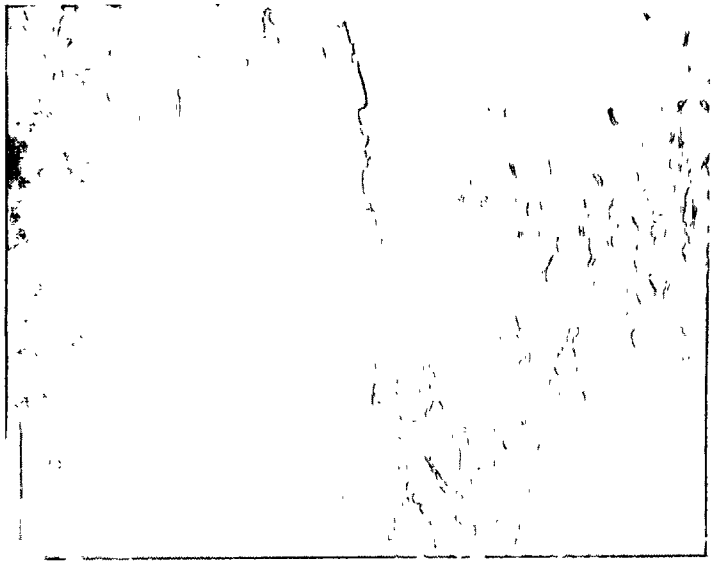

37000X

b) FINE STRUCTURE AT THE AUSTENITE-AUSTENITE GRAIN BOUNDARY

Figure 2-8. Thin Foil Transmission Electron Micrographic Showing the Fine Structure Within Austenite and Austenite-Austenite Grain Boundary

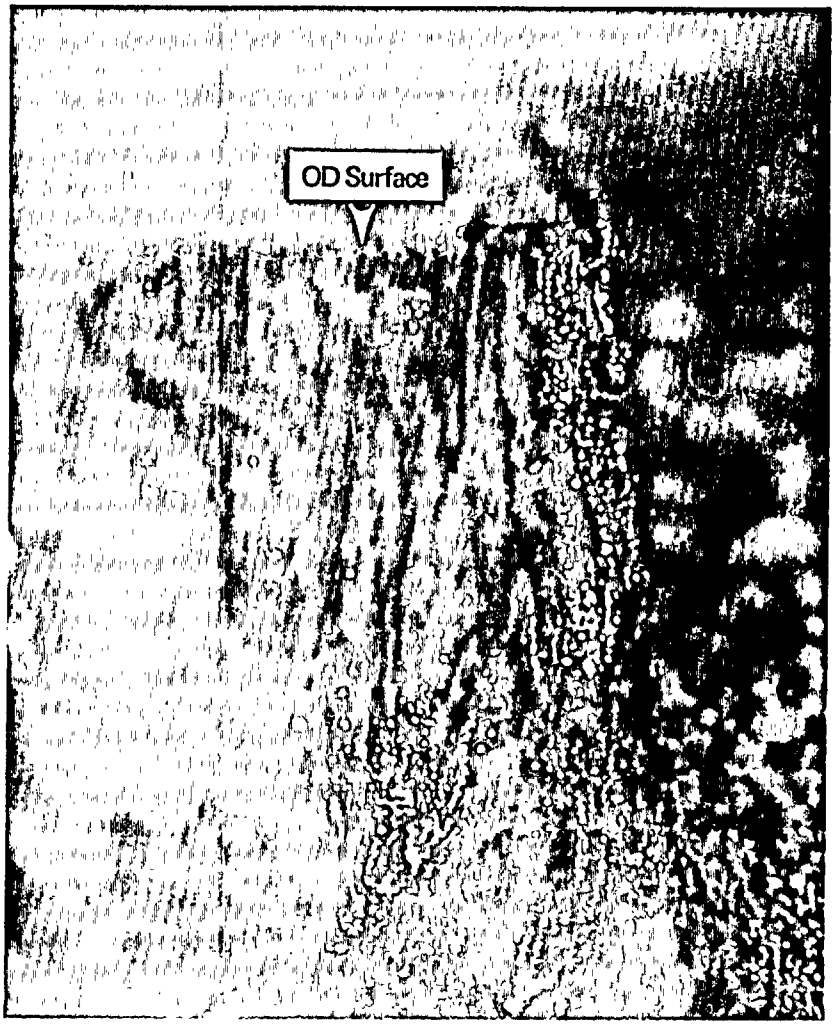

80X

Figure 2-9. Light Optic Color Photograph of Fracture Surface Showing the Intergranular Nature of Crack Path

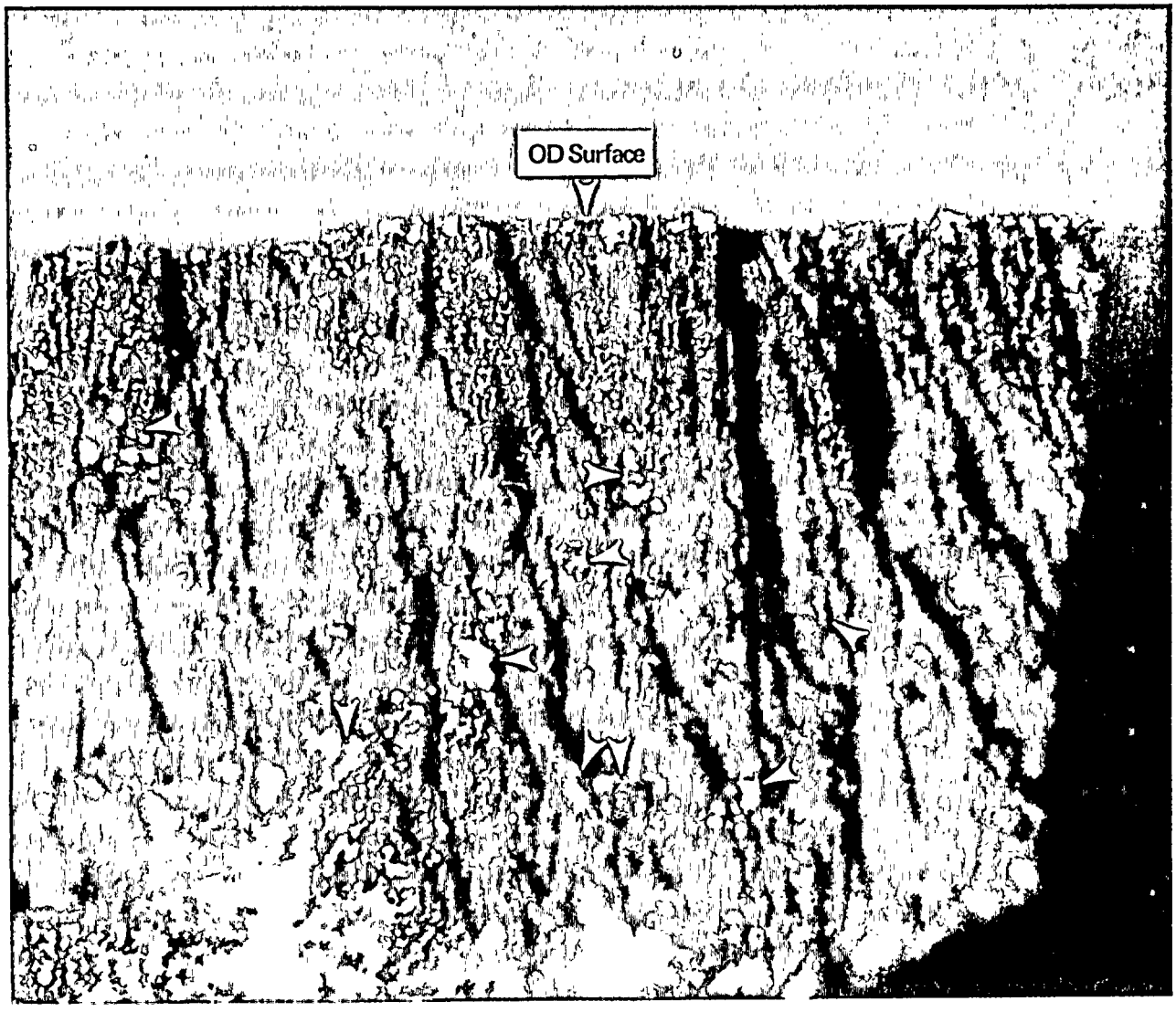

Figure 2-10. Light Optic Color Photo of Fracture Surface Showing Regions Where Laboratory Fracture Occurred

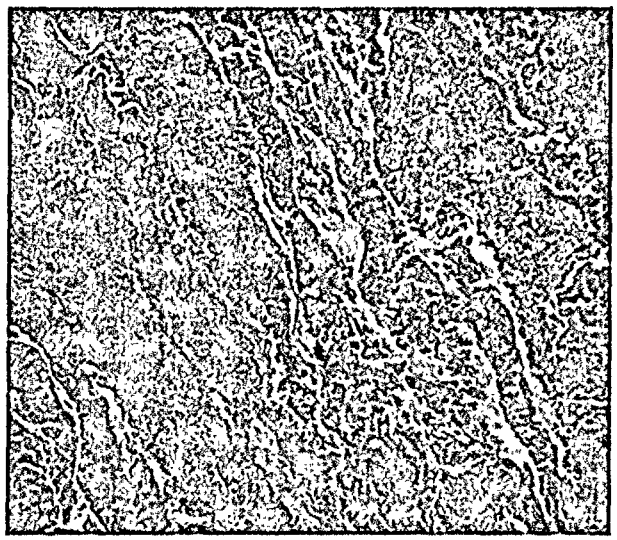

500X

500X

Figure 2-11. Scanning Electron Fractographs of the Freshly Opened Crack Surface

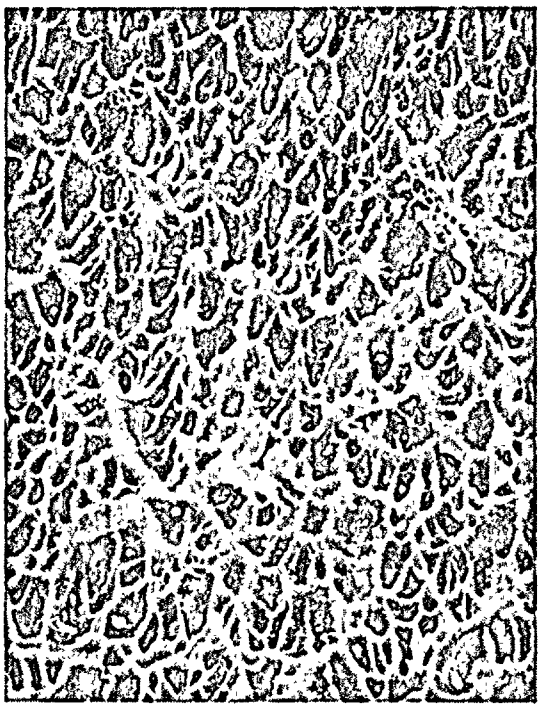

2000X

Figure 2-12. Scanning Electron Fractograph of the Laboratory Fractured Region Showing Dimpled Rupture

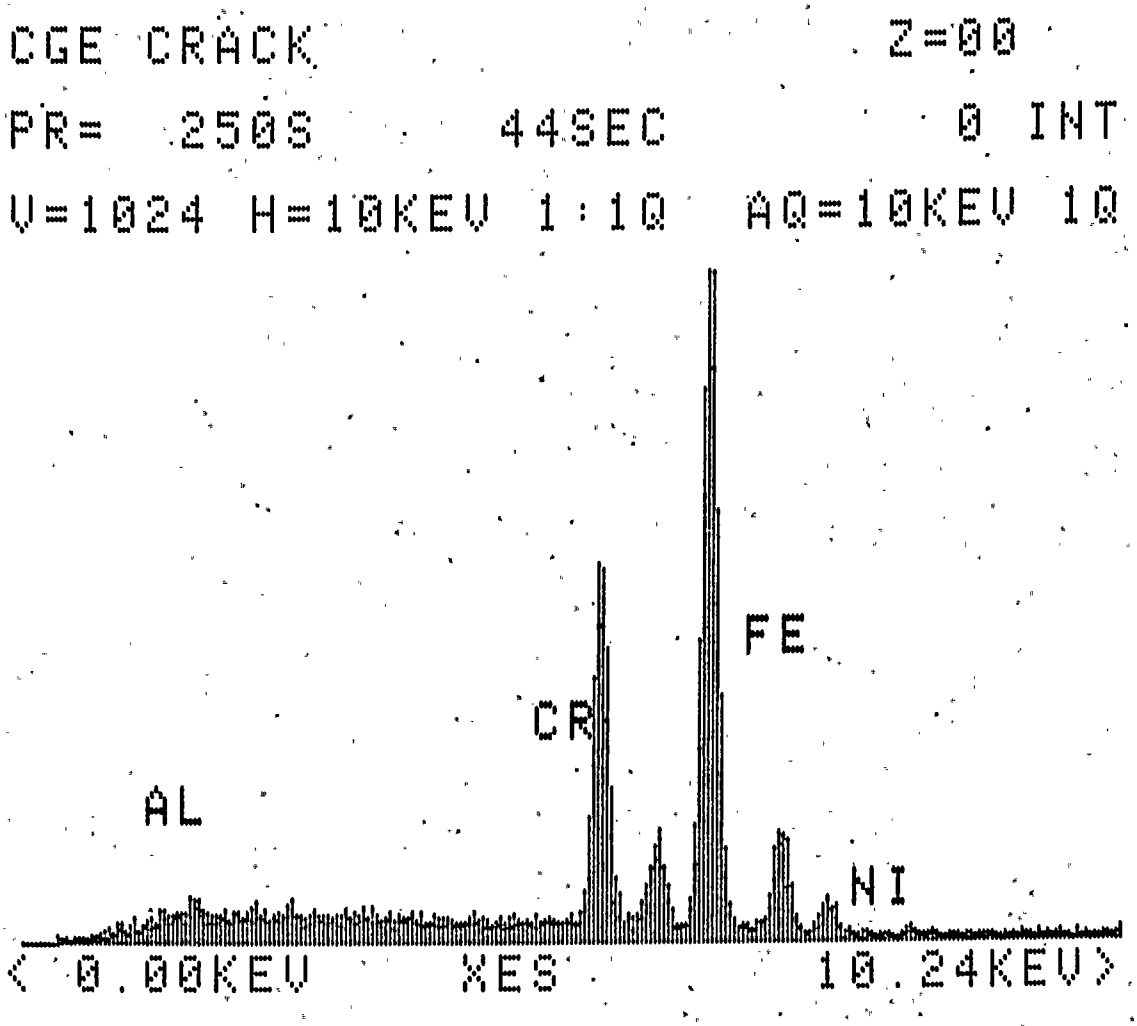

Figure 2-13. EDAX Spectrum Taken From Freshly Opened Crack Surface

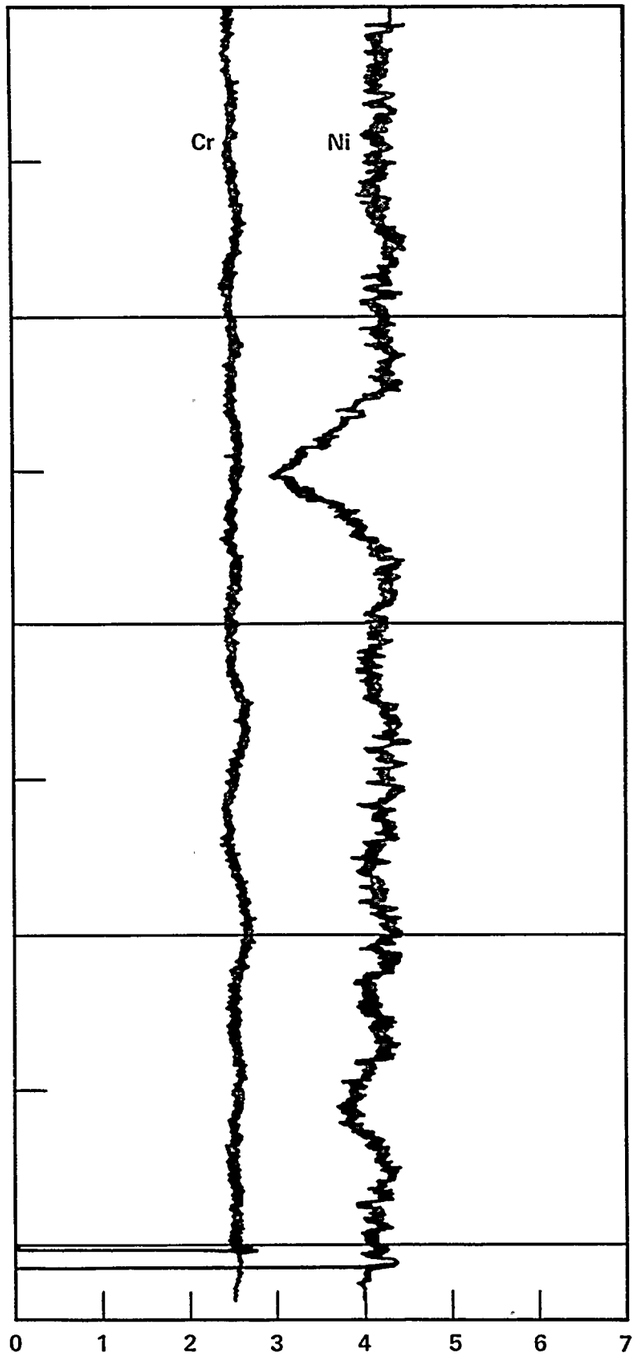

3940A

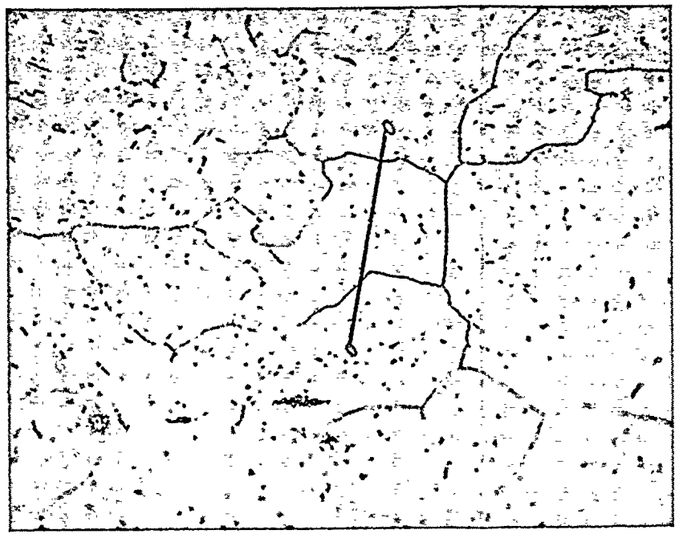

LINE TRACES #5 FOR Cr AND Ni 500X

Figure 2-14. Electron Microprobe Trace for Variation of Chromium Concentration Across Grain Boundaries

SECTION 3.0

DISCUSSION

Surface examinations of the boat sample showed that the cracks are generally oriented along the longitudinal direction of the boat sample, which corresponded to the circumferential direction of the nozzle-safe-end weld. Metallographic examination of the sections containing some of the deepest cracks showed that the cracks are intergranular in nature and extended from the OD surface of the weld metal to as deep as the base metal interface. All the cracks, however, are contained within the weld metal (figures 2-2 through 2-5), with the deepest crack measuring approximately .04 inches. The cracks appear to have been initiated at the OD surface where they appeared wider and tended to narrow down as they penetrated deeper into the weld metal. Examination of regions where some of the finer cracks appeared on the OD surface showed some evidence of cellular (interdendritic) cracking (figure 2-6). Measurements on the delta ferrite content of the weld metal by metallographic methods revealed rather low delta ferrite numbers, ranging from 2.5 percent to a maximum of 3 percent (figure 2-7). Fine structural studies by thin foil transmission electron microscopy showed no appreciable evidence of intergranular carbide precipitation (figure 2-8).

Fractographic examinations of the fracture faces by light optic color photography revealed interesting metal oxide colors indicative of the temperatures to which the crack surfaces may have been first exposed to the environment. In fact, the heavy dark surface oxide band seen at the crack mouth (shown at top of the fractograph, figure 2-10) suggests significantly higher temperatures of exposure. The color fractography also brings out a significant observation that localized pockets of cohesive weld metal islands (shown by arrows in figure 2-10) bridging the mating faces of the crack were still present within the crack, prior to laboratory fracture. Fractographic examinations by scanning electron microscopy showed no evidence of corrosion deposits. Energy dispersive x-ray analysis of the fracture faces showed no traces of corrosion products such as chlorides or sulphides (figure 2-13).

The intergranular and branching nature of the cracks, the irregular morphology of the crack faces, and the presence of cohesive islands of weld metal bridging the mating faces of the crack, all clearly point to the fact that the cracking could not have been the result of fatigue fracture, which is generally caused by the advance of a continuous crack front under cyclic loading conditions. Also, the lack of sensitized microstructure in the weld metal

(i.e., absence of appreciable intergranular carbide precipitation), and the absence of any traces of corrosion products on the freshly opened crack surfaces demonstrates that the stress corrosion could not have played any significant role in the cracking mechanism.

The heavy metal oxide films on the fracture surface revealed by light optic and color photographic studies suggest that the cracking may have occurred at significantly higher temperatures, resulting in the exposure of crack surfaces to heavy oxidation. A close examination of metallographic sections containing some of the finer cracks and the scanning electron fractrographic appearance of crack faces shows evidence of cellular cracking in the fracture process. These observations suggest that supersolidus cracking or "hot cracking" may have contributed to the fracture mechanism. Further support for this hypothesis can be sought from the significantly lower contents of delta ferrite found in the stainless steel, rendering the weld metal susceptible to hot cracking.

The term "hot cracking" used here refers to the supersolidus cracking that occurs in welds or castings during solidification. It is caused by the localized strains set up by thermal contraction under restraint, tending to pull apart solid masses (grains, cells) of material separated by thin liquid films.

The theory of hot cracking has been extensively summarized by many workers in the literature (for example, see reference 2) so that it is not necessary to go into detailed discussion here. Under the strain theory of hot cracking outlined earlier, the amount of cracking experienced is related to the amount of straining in the so-called "critical solidification range" of the freezing process. The primary reason for this is that if the grains are pulled apart by excessive straining during this critical freezing range, no healing of cracks is possible because the remaining liquid volumes are not interconnected. Thus solid-liquid interfacial energies as well as strains from external restraint play a significant role in the cracking process.

Unanimous evidence exists in the literature that delta ferrite reduces the hot cracking susceptibility of stainless steel weld deposits. Of the several reasons offered for this beneficial effect, the most commonly known theory is that ferrite has a greater solubility than austenite for certain harmful elements and impurities, and thus reduces the amount of liquid films and the temperature range over which they exists during solidification. Another explanation often suggested is the creation of a substantial interfacial area between ferrite and austenite in addition to austenite-austenite boundaries. This extra interfacial area then acts as a sink to decrease the concentration of impurities at the austenite boundaries and reduces hot cracking.

Earlier studies of the effect of delta ferrite content on the hot cracking sensitivity of stainless steel welds show that a minimum delta ferrite content of approximately 5 percent is needed to provide adequate resistance to hot cracking, while optimum resistance to hot cracking is achieved for ferrite contents in the range between 5 percent to 10 percent. Ferrite contents in excess of 10 percent may result in unfavorable distribution of ferrite in the stainless steel microstructure, reducing the resistance to hot cracking. Also at these high ferrite contents, a brittle sigma phase can form at the ferrite-austenite boundaries, embrittling the weld metal.

An examination of the nozzle-to-safe-end assembly shown in figure 1-1 suggests that the geometric discontinuity at the carbon steel/weld metal interface (where cracking was observed) can be a source of appreciable local strains arising both from the restraint of the joint assembly and from the thermal stresses generated during freezing. Thus, in the absence of adequate delta ferrite in the weld metal, it is believed that the strains generated at the carbon steel/weld metal interface induced "hot cracking" in the weld metal. The formation of high-temperature metal oxide film on the fracture faces and the various fractographic features observed by light optic and scanning electron optic methods consistently support this hypothesis. The presence of islands of cohesive material bridging the two mating faces of the crack is yet another evidence reinforcing the hot cracking argument.

SECTION 4.0

CONCLUSIONS

The cause of cracking in the pressurizer nozzle-to-safe-end weld of the Robert Emmett Ginna Nuclear Power Generating Station appears to be supersolidus cracking or "hot cracking." Inadequate delta ferrite content of the stainless steel weld metal local to the weld interface and a geometric discontinuity at the nozzle carbon steel/weld metal interface were among the contributors to the cracking process. It is also concluded that the nature of cracking is exclusive to the current incident and not generic.

REFERENCE

1. R. Rishel and J. S. Caplan Westinghouse, NTD, Trip Report No. MT-MNA-857.
2. F. C. Hull, "Effect of Delta Ferrite on the Hot Cracking of Stainless Steel," Welding Research Supplement, September 1967, p. 399-S.